International Journal of Nanomedicine

Dovepress
open access to scientific and medical research

Open Access Full Text Article

ORIGINAL RESEARCH

Nd_2O_3 Nanoparticles Induce Toxicity and Cardiac/Cerebrovascular Abnormality in Zebrafish Embryos via the Apoptosis Pathway

This article was published in the following Dove Press journal:
International Journal of Nanomedicine

Yu Chen,[1–3]* Wei Zhu,[4]* Fan Shu,[5] Yan Fan,[1,2] Ning Yang,[1,2] Tao Wu,[1,2] Le Ji,[1,2] Wei Xie,[1,2] Rengui Bade,[1,2] Shuyuan Jiang,[1,2] Xiaolei Liu,[1,2] Guo Shao,[1–3] Gang Wu,[1,2] Xiaoe Jia[1–3]

[1]Biomedicine Research Center, Neuroscience Institute, Baotou Medical College, Baotou 014040, People's Republic of China; [2]Inner Mongolia Key Laboratory of Hypoxic Translational Medicine, Baotou Medical College, Baotou 014040, People's Republic of China; [3]Beijing Key Laboratory of Hypoxic Conditioning Translational Medicine, Xuanwu Hospital, Capital Medical University, Beijing, People's Republic of China; [4]School of Pharmacy, Baotou Medical College, Baotou 014040, People's Republic of China; [5]Third Hospital of Baotou, Baotou, People's Republic of China

*These authors contributed equally to this work

Introduction: Rare-earth nanoparticles in the environment and human body pose a potential threat to human health. Although toxic effects of rare-earth nanoparticles have been extensively studied, the effects on the early development are not well understood. In this study, we attempted to explain the toxic effects of neodymium oxide (Nd_2O_3) nanoparticles on early development.

Methods: We added the Nd_2O_3 nanoparticles at different concentrations and recorded the mortality and malformation rate per 24 hrs under a microscope. The live embryos treated with Nd_2O_3 nanoparticles were imaged as movies and Z step lapses with a confocal microscope, and heart rates were counted for 30 s to measure the cardiac function. The live Tg (*Flk1*:EGFP) transgenic embryos exposed to Nd_2O_3 nanoparticles were observed under confocal microscope to measure the cerebrovascular development. Subsequently, we extracted the total protein for Western blot at 5 days post-fertilisation (dpf). Embryos were collected to undergo TUNEL staining for apoptosis detection.

Results: Nd_2O_3 nanoparticles disturbed embryo development at high concentrations (>200 μg/mL). The mortality and malformation rate gradually increased in a dose-dependent manner by morphological observation, while the Nd_2O_3 median lethal concentration (LD50) was 203.4 μg/mL at 120 hrs post-fertilisation (hpf). Furthermore, the Nd_2O_3-treated embryos showed severe arrhythmia and reduced heart rate. We also observed the markedly cerebrovascular disappearance at middle concentration (100 and 200 μg/mL). The downregulated autophagy flux in brain blood vessels and increased apoptosis level in neurons might affect vessels sprouting and contribute to the vanished cerebrovascular.

Conclusion: The results suggested that the embryos exposed to Nd_2O_3 activated the apoptosis pathway and induced toxicity and abnormal cardiac/cerebrovascular development.

Keywords: Nd_2O_3, zebrafish, toxicity, arrhythmias, cerebrovascular

Introduction

Rare earth is a strategic resource with widespread use in industry, agriculture, military industry, environmental protection and medicine. Rare-earth nanoparticles have a role in biomedical imaging[1] and anti-tumour medicine.[2] Due to the gradual exposure of nanoparticle materials to the ecological environment, rare-earth nanoparticles could enter the human body via the respiratory system and food chain, such as through water and plants.[3]

Some studies have found that rare-earth elements have cytotoxicity and genotoxicity.[4] Yb^{3+} decreased zebrafish embryo survival and hatching rate and caused tail malformation.[5] Sprague-Dawley (SD) rats treated with neodymium oxide (Nd_2O_3)

Correspondence: Xiaoe Jia
Email evangeline2004@163.com

Gang Wu
Tel/Fax +86-472-7167830
Email wugang0525@163.com

have been found to have severe lung inflammation.[6] Gold nanoparticles (AuNP) have been found to produce early embryonic development abnormalities in zebrafish.[7] In addition to studies in cells and model animals, several toxicity studies in humans have been reported. Gadolinium contrast agent can cause nephrogenic systemic fibrosis in clinical patients,[8] which is widely applied in radioactive medicine. Some workers specialising in occupations related to rare-earth exposure have suffered from diseases of the respiratory system.[9]

Nd_2O_3 nanoparticles are important earth rare materials and are widely used for making glass, capacitors and magnets.[10] However, toxicity of Nd_2O_3 nanoparticles has not been well investigated, especially in early development. As zebrafish are increasingly used as models for the toxicity examination, we selected them to evaluate the mechanism of Nd_2O_3 toxicity in early development. Zebrafish are commonly used as a high-throughput animal model in acute toxicity studies. Zebrafish eggs (1.0–1.2 mm in diameter) are transparent and develop quite rapidly, which facilitates direct observation of the toxic effects on their internal organs. Zebrafish embryos or larvae are some of the most commonly used model organisms for the toxicity examination because they are particularly sensitive to low-level environmental pollutants.[11]

The aim of the present study was to explore the effects of Nd_2O_3 nanoparticles on the early development of zebrafish embryos. Our research also tried to provide practice guidance for workers about long-term occupational health exposure and provide instructions for comprehensive evaluation of occupational health. This study demonstrated that Nd_2O_3 can induce toxic effects in a dose-dependent manner through the apoptosis pathway. The treated embryos exhibited cardiac arrhythmias and cerebrovascular development disorders.

Materials and Methods

Zebrafish Maintenance and Embryo Collection

Zebrafish (*Danio rerio*) maintenance and staging were performed as described previously.[12] Adult zebrafish were maintained in a closed flow through a culture system filled with conditioned water (pH: 7.0±1.0; temperature: 28±1°C; conductivity: 450 S/cm) and a 12h:12hr cycle of day and night. Zebrafish were fed live brine shrimps (*Artemia salina*) twice daily. The night before the experiment began, male and female fish were placed in the same hatching box and separated by a comb. The next morning, the zebrafish began to spawn at the moment of light. Viable eggs were collected and rinsed at least 3 times with E3 medium (egg water) (5 mmol/L NaCl, 0.17 mmol/L KCl, 0.33 mmol/L $CaCl_2$ and 0.33 mmol/L $MgSO_4$, pH: 7.0±1.0), which is the standard hatchery water for zebrafish eggs. To ensure the developmental synchronisation at the beginning of exposure, the embryos at approximately 2.5–3.0 hours post-fertilisation (hpf) were sorted under a stereo microscope. Healthy embryos at 8–10 hpf were then subjected to Nd_2O_3 exposure. The Tg(*Flk1*:EGFP) transgenic line was used to observe the blood vascular.

Ethics Statement

The zebrafish facility and study were approved by the Institutional Review Board of Baotou Medical College, and zebrafish were maintained according to the guidelines of the Institutional Animal Care and Use Committee.

Nd_2O_3 Treatments

The stock solution of Nd_2O_3 (USA, Sigma, 634611) nanoparticles was 50 mg/mL. Zebrafish embryos were transferred into 6-well multi-plates with 30 embryos per well. Three millilitres of E3 medium treated with different concentration Nd_2O_3 (0, 50, 100, 200, 400 and 800 μg/mL) were added to each well of 6-well multi-plates. Before adding the nanoparticles, Nd_2O_3 nanoparticles were pretreated with ultrasound equipment for 30 mins. Zebrafish embryos were exposed to different concentrations of Nd_2O_3 for 5 d in an illumination incubator at 28±1°C with the cycle of day and night, and the Nd_2O_3 was changed every 2 days.

Zebrafish Embryos Toxicity Assay

The different concentrations of Nd_2O_3 were directly observed in each well every 24 hrs under a stereo microscope (Nikon, SMZ18) connected to a camera device at specific time points (24, 48, 72, 96 and 120 hpf). The toxicological analysis included tail detachment, eye development, somite formation, circulatory system, pigmentation, hatching rate, malformations, length of larvae and mortality. After 120 hpf, larvae were anaesthetised in 0.02% tricaine and embedded in 1% low-melt agarose gel, and then the larvae were positioned on the lateral side and photographed to assess morphology. All experiments were repeated 6 times independently.

Terminal Deoxynucleotidyl Transferase dUTP Nick End Labelling (TUNEL) Staining

The 120 hpf embryos were stained using an in situ cell death detection kit (Roche, 12156792910). The zebrafish embryos were fixed overnight at 4°C in freshly prepared 4% paraformaldehyde (Fix). The next day, they were washed in phosphate-buffered saline plus Tween (PBST), and increasing concentrations of methanol were used to measure the gradient of dehydration until 100% methanol overnight at −20°C. On the third day of rehydration, the embryos were treated with Proteinase K (Sigma, P8044) for 30 mins and refixed for 1 hr. Subsequently, a TUNEL staining kit was used to stain the embryos in the dark for 3 hrs. When the staining was almost over, the staining conditions were observed with a stereo microscope to assess whether to stop reaction. After termination reaction, the embryos were observed under a confocal microscope.

Live Imaging of Autophagy in Tg(Flk1:EGFP) Transgenic Embryos

The *mCherry-Lc3* mRNA was transcribed via the mMessage mMachine SP6 kit (Ambion), and then injected into Tg(*Flk1*:EGFP) transgenic zebrafish embryos at 1-cell stage as described in our previous paper.[13] The live embryos were anaesthetised with tricaine and mounted in 1% low melting point agarose for imaging with confocal microscope (under a 20 X/0.8 NA water-immersion objective).

Confocal Scanning

The live embryos were anaesthetised with tricaine and mounted in 1% low melting point agarose for imaging with Nikon A1+ confocal microscope. The real-time lapse movies and Z steps were collected, and heart rates were counted for 30 s and then multiplied by 2 to calculate the heart rate in beats per minute (bpm).

Western Blot Analysis

Briefly, embryos exposed to different concentrations of Nd_2O_3 for 5 d were collected, and the yolk membranes were removed. The same volume of RIPA was added to each group of embryos, then ultrasonic crushing to collected the total protein. Protein samples were separated using 12% or 15% sodium dodecyl sulphate polyacrylamide gel electrophoresis (SDS-PAGE) and transferred to polyvinylidene difluoride (PVDF) membranes (Roche). Then, they were blocked at room temperature (RT) with 5% non-fat dry milk for 1 hr. The membranes were incubated with primary antibodies at a dilution of 1:1000 overnight at 4°C. Primary antibodies included antibody *cleaved-caspase 3* (CST, 9661), antibody *Lc3* (CST, 4108), antibody *P53* (CST, 2524), antibody *Bcl-2* (CST, 2772) and antibody *α-tubulin* (Sigma, T6199). The next morning, the membranes were incubated with horseradish peroxidase-conjugated secondary antibodies at RT for 1 hr and finally immunoreactive signals were detected by Immobilon Western Chemiluminescent HRP substrate (Millipore, WBKLS0500). To ensure the feasibility of the experiments, the experiments were repeated at least 3 times.

Statistical Analysis

All data were statistically analysed using the two-tailed Student's *t*-test with GraphPad Prism 5 software. When $P<0.05$, the difference was statistically significant. All values were reported as the mean ± standard and the data analysis of at least 3 replicate measurements with at least 3 batches of different and independent samples.

Results

Nd_2O_3 NPs Can Be Ingested by Zebrafish

Wild-type embryos exposed to Nd_2O_3 NPs for 120 hrs were imaged using a confocal microscope to determine the uptake of nanoparticles in 2 living zebrafish. In vivo time-lapse imaging (Figure 1) showed that Nd_2O_3 NPs were present inside the digestive tract. Nd_2O_3 NPs were moved with intestinal movement from 1.798 s (Figure 1A) to 20.653 s (Figure 1E) and from 11.892 s (Figure 1F) to 29.548 s (Figure 1J). Whole time-lapse imaging also can be seen in Supplementary Movie S1.

The Mortality of the Larvae Treated by Nd_2O_3 Increased in a Dose-Dependent Manner

To explore its direct toxicity, we recorded the number of dead embryos after treatment with Nd_2O_3 nanoparticles for 5 d. Compared with the untreated group (control), low concentrations (50 and 100 μg/mL) of Nd_2O_3 had nearly no toxicity, and high concentrations caused significant toxic effects. The embryos of mortality were 100% (Figure 2A) at the concentration of 800 μg/mL, and the median lethal concentration (LD50) was 203.9 μg/mL. In addition, the mortality of the larvae increased in a dose-dependent manner (Figure 2A).

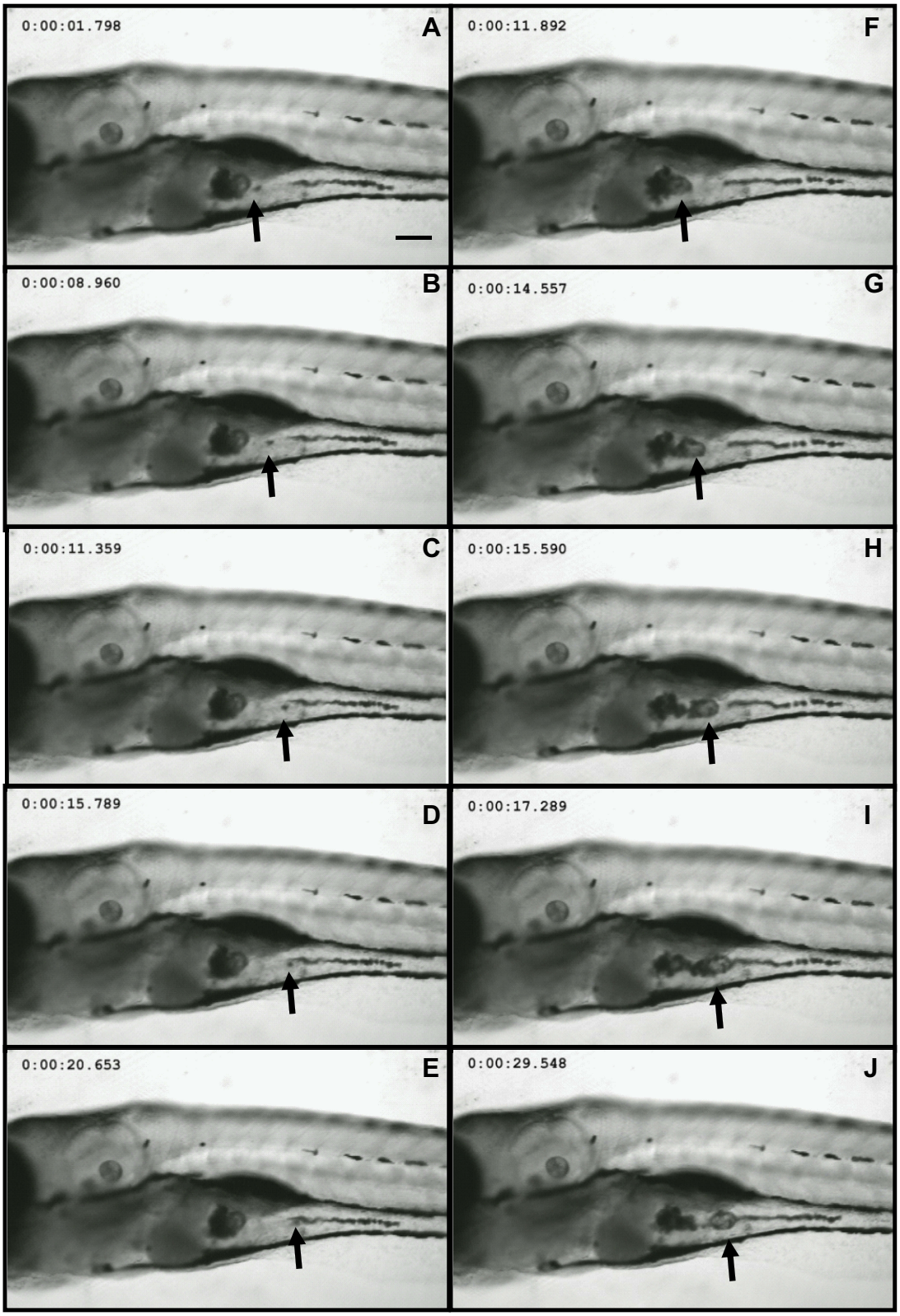

Figure 1 Nd_2O_3 nanoparticles can be ingested by zebrafish. Representative confocal images are shown. (**A**–**E**) and (**F**–**J**) show Nd_2O_3 trajectory images in the digestive tract of two zebrafish embryos. Black arrows indicate the Nd_2O_3 particles. Whole time-lapse imaging can be seen in Supplementary Movie S1.

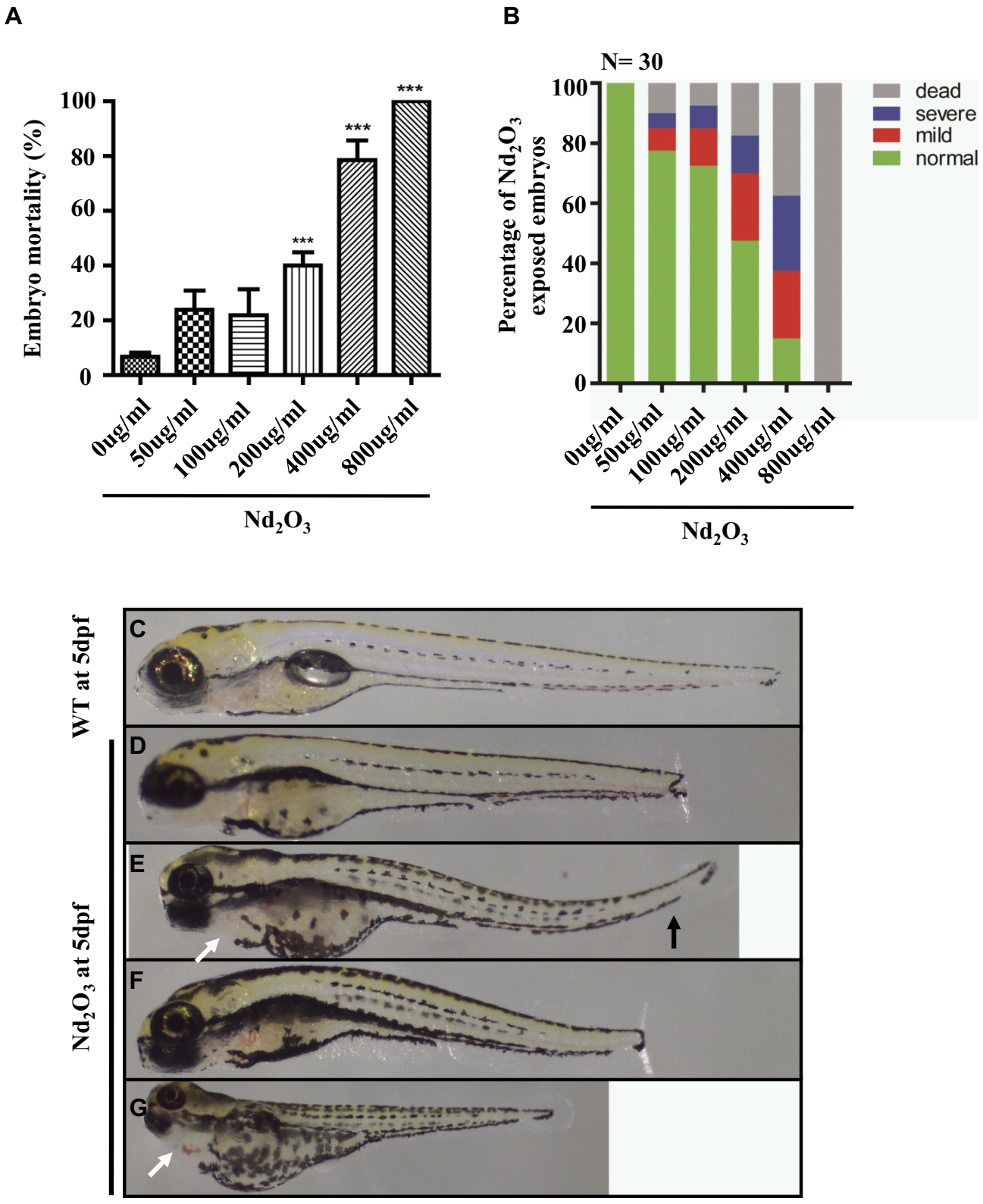

Figure 2 Effects of Nd_2O_3 on the mortality and malformation of larvae at 120 hpf. (**A**) The mortality of the larvae increased in a dose-dependent manner. Compared with the 0 ug/mL group. ***$P \leq 0.001$ (Student *t* test). (**B**) The percentage of abnormal embryos treated with Nd_2O_3. These experiments were repeated at least 3 times. (**C**) Light microscope image of zebrafish wild-type (WT) embryos at 5 dpf. (**D–G**) Light microscope images of embryos treated with Nd_2O_3 at 5 dpf. Black arrows indicate bent tail. White arrows indicate cardiac oedema.

Nd_2O_3 Mediated Malformation in Zebrafish Embryos

Subsequently, we found that Nd_2O_3 of different concentrations could cause different levels of malformation. There are 3 main malformation types, including decreased body length (Figure 2D), bent tail (Figure 2E and F) and cardiac oedema (Figure 2G). To further explore the toxicity effect of Nd_2O_3 nanoparticles, we recorded the ratio of the embryo malformation, which increased in a dose-dependent manner (Figure 2B).

The Heart Rate of Embryos Treated with Nd_2O_3 Was Reduced

Cardiac performance was assessed using confocal real-time recording, which revealed an overall reduction in heart rate. Robust rhythmic contractions were observed in atrium and ventricle in control (0 μg/mL) embryos. Upon exposure to 200 μg/mL Nd_2O_3, some problems were detected with the heartbeat. The heart rate of 10–30% treated embryos reduced (Figure 3A). The mean heart rate of control embryos at 120 hpf equals 96 beats per minute (bpm), while the mean heart rate of Nd_2O_3 exposed embryos equals 72 bpm (Figure 3B). Whole time-lapse imaging can be seen in Supplementary Movies S2–3.

Heart Dysfunction (Arrhythmia) Can Be Recorded in Embryos Exposed to Nd_2O_3

The cardiac arrhythmia phenotypes can also be observed in Nd_2O_3-treated embryos. An irregular pause can be recorded in nearly 10% of the embryos (Figure 3C). The longest pause was 7 s in Nd_2O_3-exposed embryos (Figure 3C). Whole time-lapse imaging can be seen in Supplementary Movies S4–5.

Nd_2O_3 Disturbed Cerebrovascular Development

Tg(*Flk1*:EGFP) embryos were exposed to different concentrations of Nd_2O_3 nanoparticles for 5 d, and the development of zebrafish brain blood vessels was observed using confocal microscope. For the control (untreated Tg (*Flk1*:EGFP) embryos), Figure 4A, B and 4B', the cerebrovascular of wild-type embryos was very complicated, but a large number of blood vessels of the treatment group had vanished at 5 days post-fertilisation (dpf, Figure 4C, D and D', E, F and F'). Whole time-lapse imaging can be seen in Supplementary Movies S6–7. Then, the time point was moved ahead at 4dpf and 3dpf. The cerebrovascular of treated embryos was disappeared at 4 dpf in Supplementary Figure S2. At 3dpf, there was no obvious reduced cerebrovascular (Supplementary Figure S1). However, the cerebrovascular distribution and arrangement had some abnormalities when observed in each Z-step (5 μm for one step) at 3 dpf. In wild-type embryos, the vessels appeared as pipes or lines (Figure 5A–C), while the vessels appeared as more discontinuous dots in Nd_2O_3-exposed embryos (Figure 5D–I). The cerebrovascular was developed beginning shortly after the onset of circulation at 1 dpf. The basic pattern of the vasculature was developed mostly intact nearly 7 days. The Nd_2O_3 might disturb cerebrovascular development and affect vascular sprouting. Whole Z-steps lapse imaging can be seen in Supplementary Movies S8, S9 and S10.

The Role of Autophagy and the Apoptosis Pathway in Nd_2O_3-Treated Embryos

To further validate the cause of reduced brain blood vessels, the autophagy and apoptosis evaluation was performed. To evaluate the autophagy level, immunoblotting was carried out using an antibody against the autophagy marker microtubule-associated protein light chain 3 (*Lc3*). The *Lc3* Western blot indicated that the autophagy level did not change (Figure 6A). To directly observe the autophagy level in Nd_2O_3-treated embryos, *mCherry-Lc3* synthetic mRNA was injected into Tg(*Flk1*:EGFP) transgenic zebrafish embryos at 1-cell stage, which were used as in our previous paper.[13] At 3 dpf, wild-type (WT) zebrafish embryos (Figure 6B–D) exhibited abundant *Lc3-II* puncta (indicating autophagosomes) in EGFP+ cells (the brain blood vessels). Abundant *Lc3-II* puncta in EGFP+ cells did not change at 100 μg/mL Nd_2O_3 exposure (Figure 6E–G). However, abundant *Lc3-II* puncta in EGFP+ cells decreased significantly at 200 μg/mL (Figure 6H–J) (P=0.0095, Figure 6K).

The TUNEL staining applied in embryos exposed to Nd_2O_3 nanoparticles (Figure 7A–I). The results indicated that embryos exposed to Nd_2O_3 nanoparticles have marked increased red spots on the head compared with control. We also found that the embryos exposed to medium concentrations (100 and 200 μg/mL) were more obvious than other groups (Figure 7D–I). Then, the immunoblotting against apoptosis markers was carried out to check the apoptosis pathway. The level of *cleaved caspase 3* was dramatically upregulated in embryos with Nd_2O_3 nanoparticles (100 and 200 μg/mL) (Figure 7L), and the *Bax*

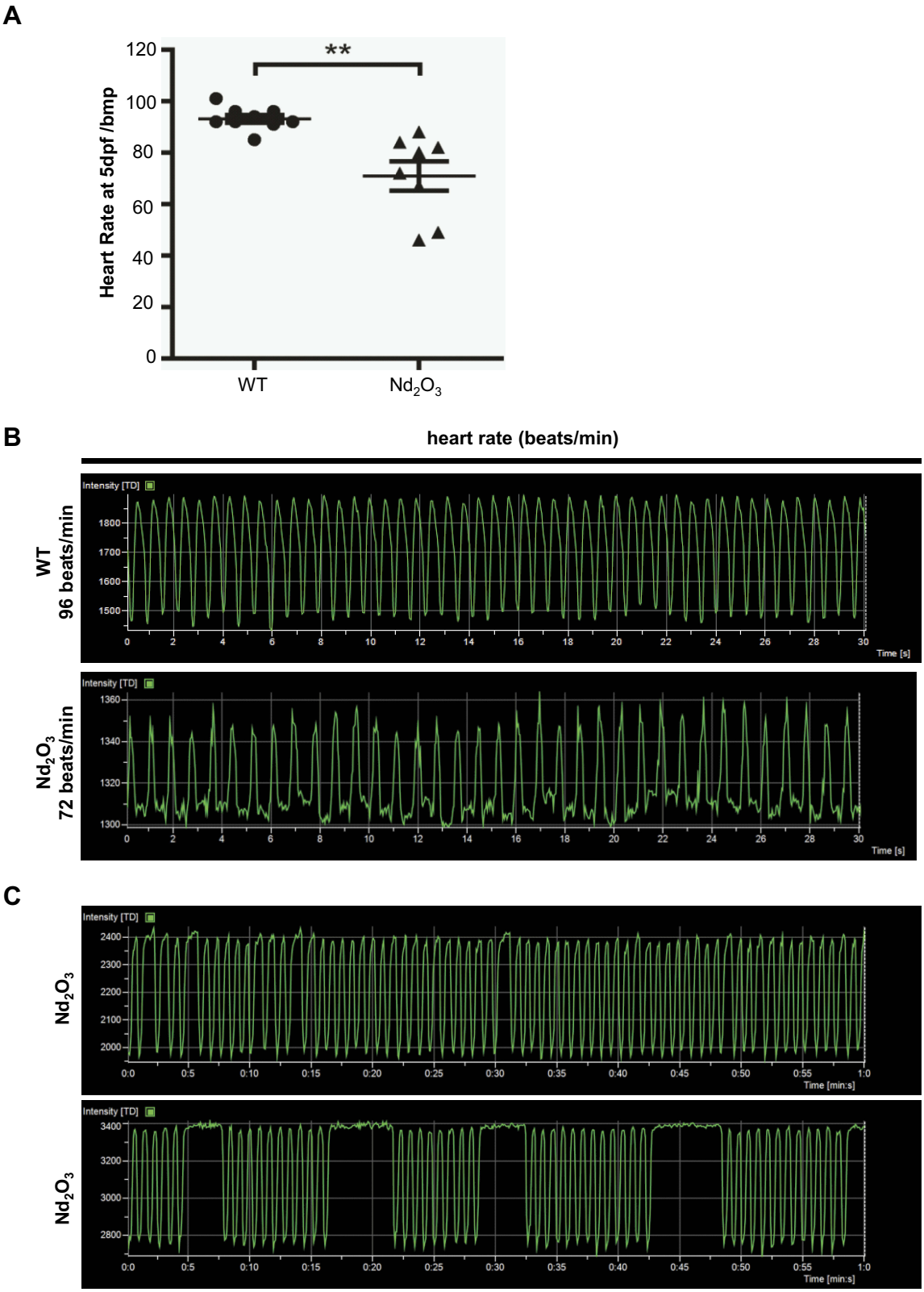

Figure 3 Nd_2O_3 contributed to reduced heart rate and arrhythmia in zebrafish embryos. (**A**) Quantitative analysis of heart rate at 5 dpf. Compared with the 0 ug/mL group. **$P \leq 0.01$. (**B**) Representative results of heart rate analysis. (**C**) Representative results of arrhythmia analysis of Nd_2O_3 exposed embryo. Whole time-lapse imaging can be seen in Supplementary Movies S2–S5.

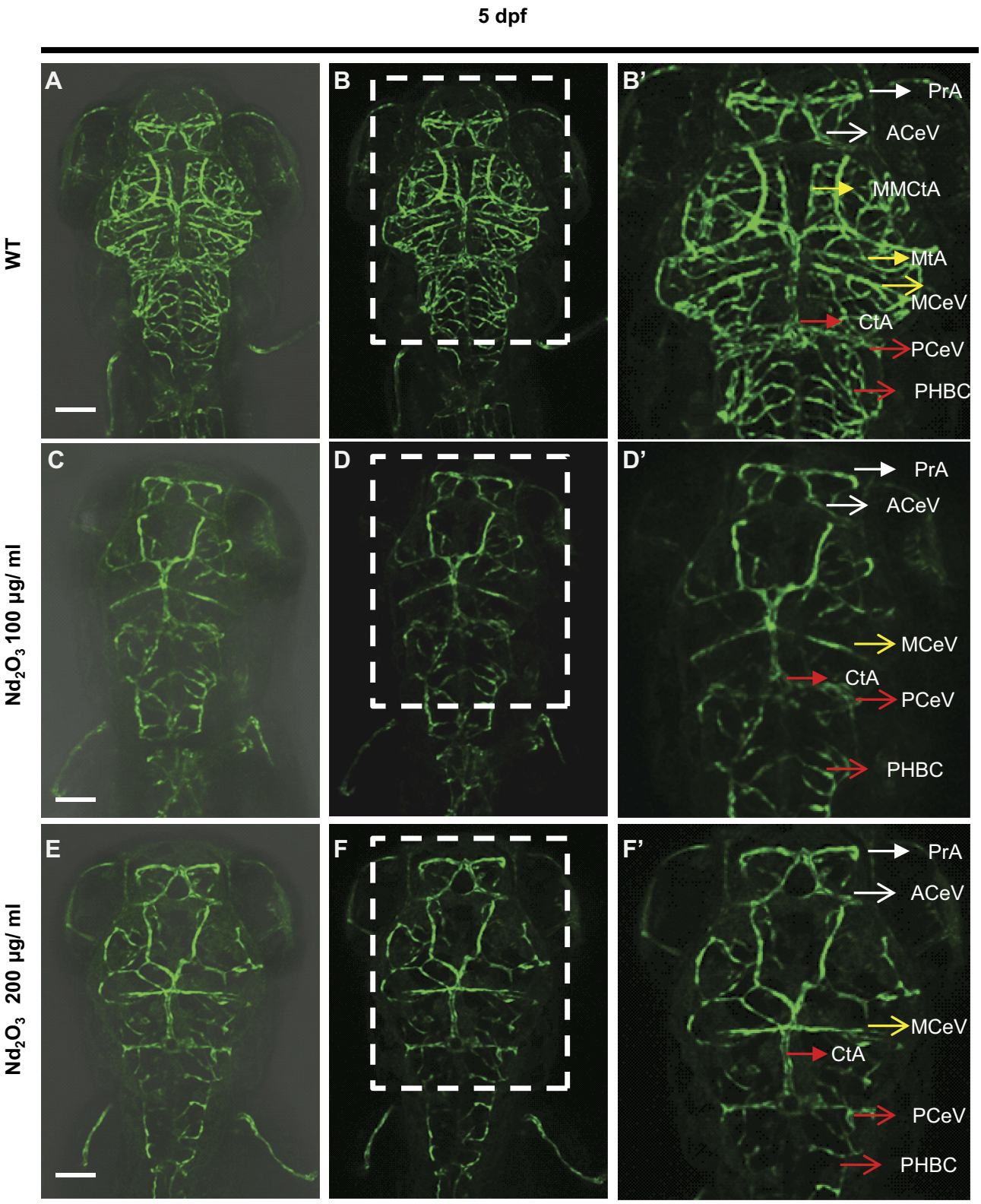

Figure 4 Nd_2O_3 disturbed the development of cerebrovascular at 5 dpf. (**A, B, B'**) The cerebrovascular images of wild-type embryo. (**C, D, D'**) The cerebrovascular images of embryos exposed to Nd_2O_3 (100 μg/mL). (**E, F, F'**) The cerebrovascular images of embryos exposed to Nd_2O_3 (200 μg/mL). Whole time-lapse imaging can be seen in Supplementary Movies S6–7. Scale bars, 100 μm.

Abbreviations: PrA, prosencephalic artery (white arrow); ACeV, anterior (rostral) cerebral vein (white arrowhead); MCeV, middle cerebral vein (yellow arrowhead); CtA, central artery (red arrow); PCeV, posterior (caudal) cerebral vein (red arrowhead); PHBC, primordial hindbrain channel (red arrowhead); MMCtA, middle mesencephalic central artery (yellow arrow); MtA, metencephalic artery (yellow arrow).

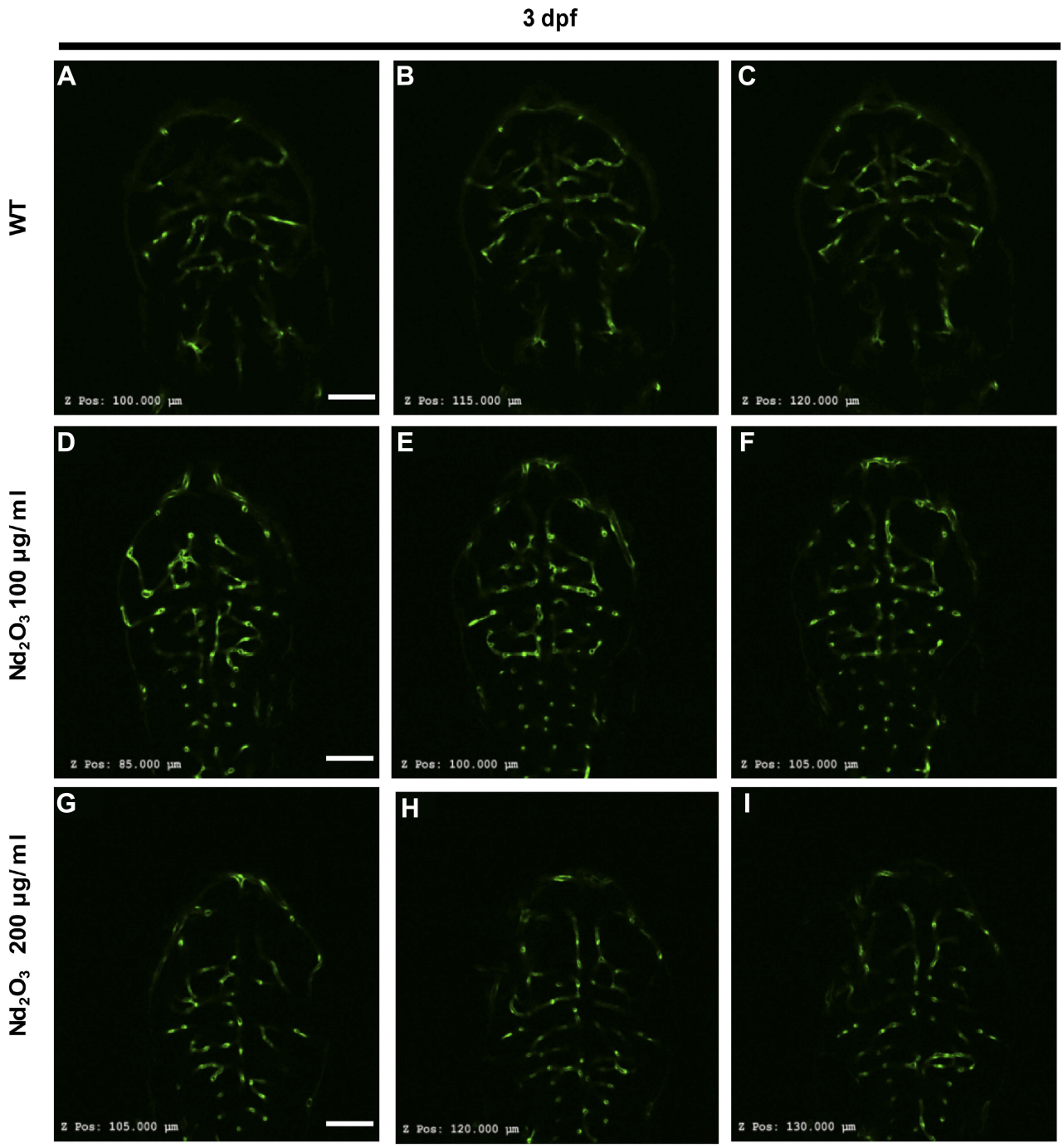

Figure 5 Nd_2O_3 disturbed vascular sprouting at 3 dpf. (**A–C**) The cerebrovascular images of wild-type embryo. (**D–F**) The cerebrovascular images of embryos exposed to Nd_2O_3 (100 μg/mL). (**G–I**) The cerebrovascular images of embryos exposed to Nd_2O_3 (200 μg/mL). Whole Z-steps lapse imaging can be seen in Supplementary Movies S8, S9 and S10. Scale bars, 100 μm.

protein increased in a dose-dependent manner (Figure 7J), while the *p53* protein increased at 50, 100 and 200 μg/mL and then reduced (Figure 7K). The *Bcl-2* was exactly opposite, first falling at 100 and 200 μg/mL and then rising at 400 μg/mL (Figure 7J). This suggested that the apoptosis pathway may contribute to Nd_2O_3 nanoparticle toxicity.

Discussion

This study demonstrated that Nd_2O_3 can induce toxic effects at high concentrations (>200 μg/mL), disturbing normal embryo development. The mortality and malformation rate was increased in a dose-dependent manner. The treated embryos exhibited cardiac arrhythmias: the

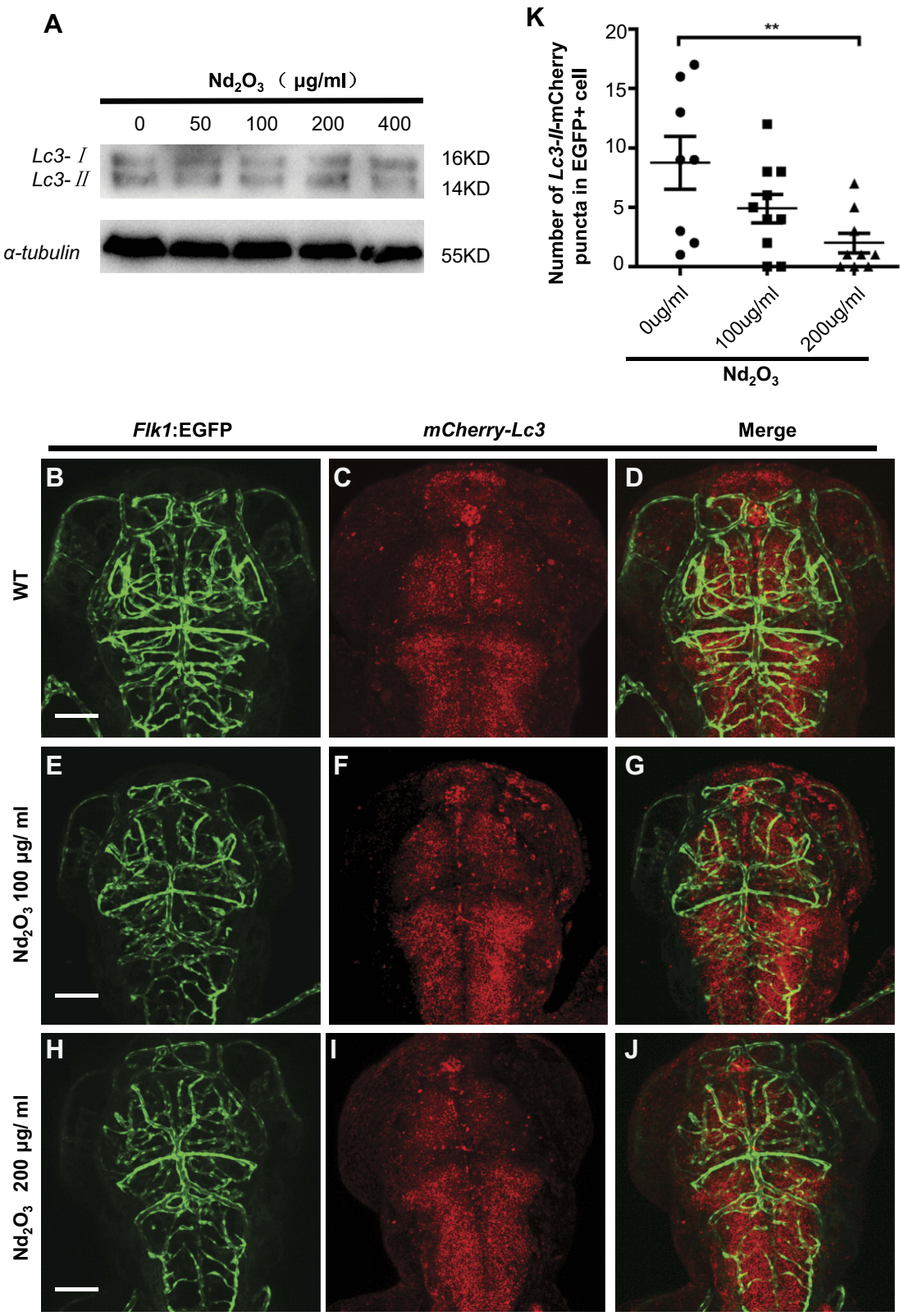

Figure 6 The autophagy level was checked in Nd_2O_3 treated embryos. (**A**) Immunoblot analysis with autophagy marker *Lc3*. (**B–J**) Representative confocal images of *mCherry–Lc3* puncta (autophagosomes) in Tg(*Flk1*:EGFP) live embryos. (**K**) Quantitative results were summarised in (**B–J**). *mCherry–Lc3* puncta were counted in EGFP+ cells in 7–10 individual embryos. Error bars in (**K**) represent standard error of the mean (SEM). $^{**}P \leq 0.01$ (Student's *t*-test). Scale bars, 100 μm.

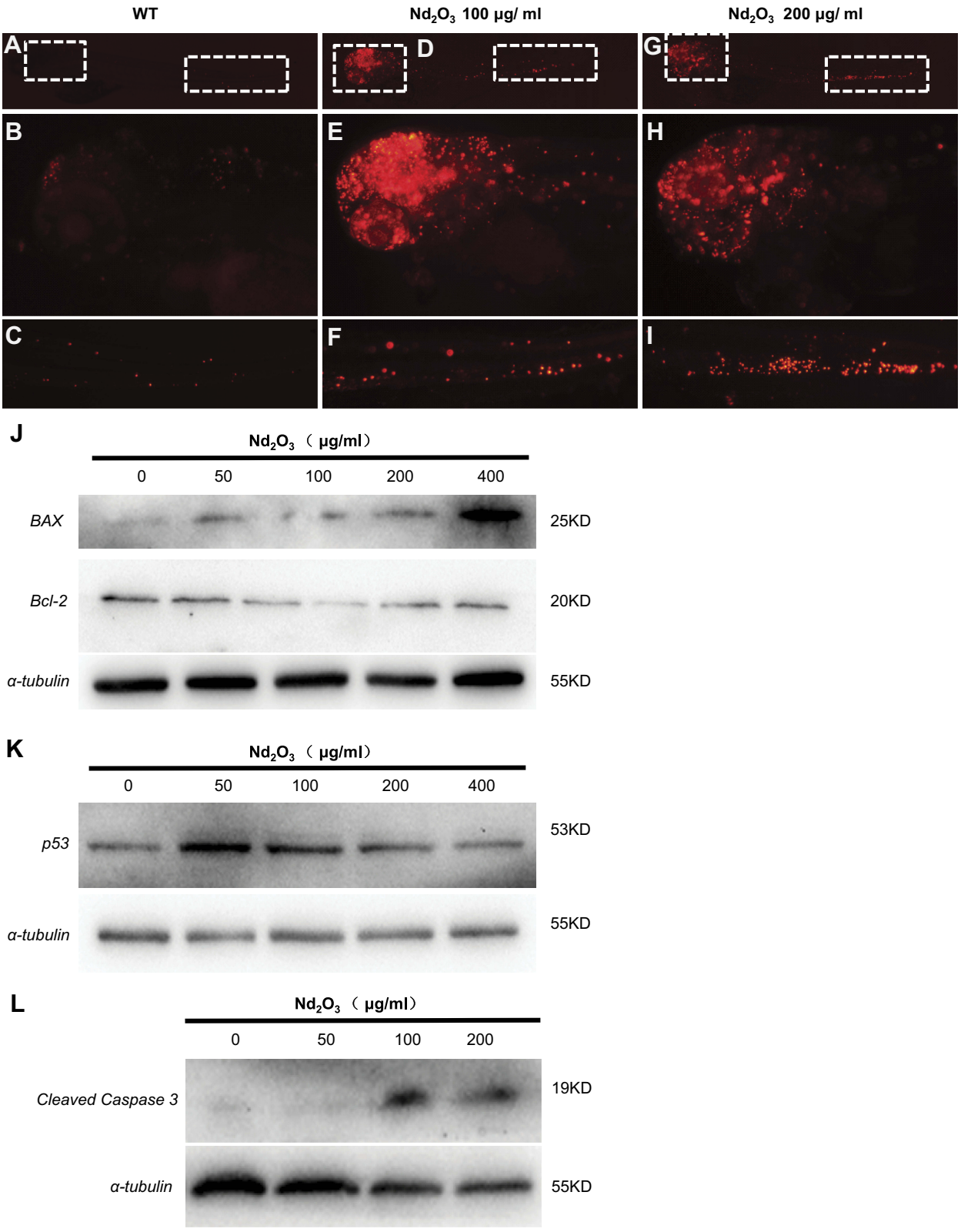

Figure 7 The apoptosis pathway was activated in Nd_2O_3-treated embryos. (**A–I**) The TUNEL staining of Nd_2O_3-treated embryos. (**A–C**) Representative images of WT embryos are shown. (**D–F**) Representative images of 100 μg/mL Nd_2O_3 treated embryos are shown. (**G–I**) Representative images of 200μg/mL Nd_2O_3-treated embryos are shown. (**J**) Immunoblot analysis with apoptosis marker *Bax* and *Bcl-2*. (**K**) Immunoblot analysis with apoptosis marker *p53*. (**L**) Immunoblot analysis with apoptosis marker *cleaved caspase 3*.

heart beat slowed down and became irregular and cerebrovascular development disorders were observed. The toxicity of Nd_2O_3 may be due to the activation of the apoptosis pathway. The downregulated autophagy flux in cerebrovascular vessels might affect vessel sprouting and contribute to the vanished cerebrovascular.

The chorion of zebrafish embryos has pore canals 500 to 700 nm in diameter that may be permeable to nanoparticles. In some studies, the nanoparticles were found to enter embryos via chorionic pore canals. The silver and gold nanoparticles passively diffused into the embryo and stayed in the embryo until hatching.[14,15] Similar to the above studies, we observed that Nd_2O_3 nanoparticles can be taken in by zebrafish (Figure 1).

In 2012, Cui et al found that the rare-earth elements La and Yb can cause zebrafish malformation and decreased hatching rate, and Yb^{3+} induced more serious toxic effects than La^{3+} in the tail in a dose-dependent manner.[5] Gold nanoparticles induced abnormal oedema and a delay in the development of the eye and head and in the onset of pigmentation.[7] Abnormal embryos were also observed in our research, including tail deformity, tail shortening and abnormal oedema (Figure 2C–G), and the embryo mortality and malformation rate increased with the increase of the concentration (Figure 2B), which is consistent with previous studies. However, embryos exposed to Nd_2O_3 showed no delay in the onset pigmentation and hatching rate in this study. As early as in 2000, some researchers found that the marine species embryos and skeletal development was restricted after 24-hr and 48-hr exposure to the rare-earth element Gd.[16,17] This malformation may be related to the skeletal development. According to these studies, the malformation caused by Nd_2O_3 nanoparticles could be related to skeletal development.

One of the most important types of drug toxicity is cardiotoxicity, which is often characterised by impaired cardiac contractility or arrhythmias. Impaired cardiac contractility or induced arrhythmias (Figure 3B and C) can cause abnormal oedema (Figure 2E and G). The heart rate was reduced when embryos were exposed to water effluents from oil/gas condensate. Gold nanoparticles induced abnormal oedema.[7] The previous research indicated that the depolarisation of smooth muscle cells was blocked with rare-earth Gd^{3+}.[18] Some studies have reported that the rare-earth element Gd^{3+} affects the contractility and electrophysiology of cardiac myocytes in divided rat heart.[19] These causes confirm the Nd_2O_3 nanoparticle cardiotoxicity in zebrafish.

Furthermore, our study found the brain blood vessels in Nd_2O_3-treated embryos disappear (Figures 4 and 5). Some studies have indicated that rare-earth nanoparticles were involved in angiogenesis, including cerebrovascular angiogenesis.[20] CeO_2 nanoparticles have been reported to inhibit vascular endothelial growth factor (VEGF)-induced capillary tube formation, and the nanoparticles induced apoptosis and proliferation of endothelial cells.[21] The reactive oxygen species (ROS) also could inhibit angiogenesis, while Nd_2O_3 nanoparticles could induce production of ROS. This may be an important reason for the disappearance of cerebrovascular in Nd_2O_3-treated embryos.

To further explain the phenomenon of vascular disappearance, we observed embryos treated with Nd_2O_3 at 3 dpf. The cerebrovascular structure of wild-type Tg(*Flk1*:EGFP) transgenic embryos was overall integrated (the vessels showed like pipes or lines). To our surprise, the cerebrovascular arrangement structure (Figure 5) differed extremely from the untreated group (the vessels showed more discontinuous dots). Along with these clues, we detected autophagy and apoptosis using microinjection *mCherry-Lc3* mRNA and TUNEL staining on the third day. We found that autophagy in cerebrovascular was downregulated in the 200 μg/mL group (Figure 6K); however, in whole embryos, there was no change. Several studies have shown that decreased autophagy could inhibit pathways involved in angiogenesis[22] and autophagy triggered angiogenesis by activating VEGF and AKT.[23] Therefore, we hypothesised that the reduced autophagy level in cerebrovascular might contribute to cerebrovascular disappearance.

However, there were other reasons for vascular disappearance. Some researchers considered that axonal trajectories of neurons correlated with blood vessel sprouting and formation of vascular networks.[24,25] Previous research indicated that the drug ceramide disturbed primary and middle primary (CaP and MiP) axonal ectopic branches or abnormal blood vessels and caused shutoff of vessel sprouting, leading to vessel disappearance. Moreover, the latest research revealed that the nervous system and tissue could affect development of vascular endothelial cells.[26] Consistent with these studies, our study observed apoptosis activated in neurons in embryos exposed to Nd_2O_3. Therefore, we hypothesised that neuronal cell death might indirectly affect angiogenesis and sprouting.

To evaluate the toxic mechanism, we focused on changes in protein levels mainly from apoptosis and autophagy. The previous study found that Nd_2O_3 nanoparticles may induce cell apoptosis and acute inflammation in low concentrations.[27] Several studies have documented that cell autophagy could be upregulated by nanoparticles in many cell lines, such as

human GBM tumour cell lines (U-87 MG),[28] HeLa cells[29,30] and tobacco BY-2 cells. Gd nanoparticles can also induce autophagy at 24 hpf and 48 hpf in paracentrotus lividus sea urchin embryos.[17] However, our experiments showed no significant changes in autophagy in whole embryos (Figure 6). The autophagy also did not change in rats treated with low concentrations of ceria oxide (CeO_2) nanoparticles[31] in some studies. Therefore, we hypothesised that the autophagic flux may be regulated in different concentrations and different models in vivo and in vitro.

Subsequently, we further focused on apoptosis. CeO_2 nanoparticles suppressed *p53* expression and amplified the autophagy flow.[32] In contrast, in our study, the *p53* expression rose (Figures 6A and 7K). Gadolinium oxide (Gd_2O_3) nanoparticles induced cell apoptosis by *BAX* and *Bcl-2* protein expression.[33] Our results demonstrated that *Bcl-2* downregulated only at low concentrations (50, 100 and 200 μg/mL). Similarly, the rats exposed to CeO_2 exhibited apoptosis via increasing *Bax*/*Bcl-2* ratio.[34] The *cleaved caspase 3* is an important apoptosis marker. Our study suggested that Nd_2O_3 nanoparticles increased *cleaved-caspase 3* expression at different concentrations.

There are some limitations for this research. First, the study did not explain how the specific pathway induced toxicity. This study does not answer the question of whether the slight ionisation phenomena of Nd_2O_3 nanoparticles causes effects in zebrafish embryos. Therefore, the study aimed to provide the practice guidance for nano miners, workers related to nanomaterial fabrication, patients and pregnant women in occupational health protection. At the same time, the study provided instructions for comprehensive evaluation of occupational health.

Conclusion

Nd_2O_3 nanoparticles disturbed embryo development at high concentrations (>200 μg/mL). The mortality and malformation rate of the embryos treated with Nd_2O_3 increased in a dose-dependent manner. Furthermore, the Nd_2O_3-treated embryos exhibited severe arrhythmia and reduced heart rate. The cerebrovascular vessels partly disappeared at middle concentration (100 and 200 μg/mL). The downregulated autophagy flux in cerebrovascular vessels and increased apoptosis level in neurons might affect vessels sprouting and contribute to the vanished cerebrovascular. The toxicity of Nd_2O_3 on zebrafish embryos was induced by the activated apoptosis pathway.

Highlights

1. Nd_2O_3 nanoparticles disturbed embryo development in a dose-dependent manner.
2. Nd_2O_3 nanoparticles resulted in the disappearance of cerebrovascular vessels.
3. Nd_2O_3 nanoparticles activated the apoptosis pathway and induced toxicity.

Acknowledgments

This work was supported by the National Natural Science Foundation of China under grants 81660204, 81901918, 81550038, and 81160341, Inner Mongolia Science Foundation under grant 2019MS08060, Inner Mongolia High School Science Research Foundation under grant NJZY16207, Baotou Medical College Foundation under grant BYJJ-YF 201610, Young Talents of Science and Technology in Universities of Inner Mongolia Autonomous Region under grant NJYT-17-B32, Innovative and Entrepreneurial Talents in the "Prairie Talents" Project of Inner Mongolia Autonomous Region under grant Q2017047, and Inner Mongolia College Students Innovative Training Programme under grant 201610127, S201710127(Y01). We thank Hou Lin, Xue Zhihong (Nikon engineer) for technical support and suggestions.

Disclosure

The authors report no conflicts of interest in this work.

References

1. Liu C, Hou Y, Gao M. Are rare-earth nanoparticles suitable for in vivo applications? *Adv Mat*. 2014;26(40):6922–6932. doi:10.1002/adma.v26.40
2. Liang XJ, Meng H, Wang Y, et al. Metallofullerene nanoparticles circumvent tumor resistance to cisplatin by reactivating endocytosis. *Proc Natl Acad Sci U S A*. 2010;107(16):7449–7454. doi:10.1073/pnas.0909707107
3. Turra C. Sustainability of rare earth elements chain: from production to food - a review. *Int J Environ Health Res*. 2018;28(1):23–42. doi:10.1080/09603123.2017.1415307
4. Franchi LP, Manshian BB, de Souza TA, et al. Cyto- and genotoxic effects of metallic nanoparticles in untransformed human fibroblast. *Toxicol in Vitro*. 2015;29(7):1319–1331. doi:10.1016/j.tiv.2015.05.010
5. Cui J, Zhang Z, Bai W, et al. Effects of rare earth elements La and Yb on the morphological and functional development of zebrafish embryos. *J Environ Sci*. 2012;24(2):209–213. doi:10.1016/S1001-0742(11)60755-9
6. Kim YS, Lim CH, Shin SH, Kim JC. Twenty-eight-day repeated inhalation toxicity study of nano-sized neodymium oxide in male sprague-dawley rats. *Toxicol Res*. 2017;33(3):239–253. doi:10.5487/TR.2017.33.3.239
7. Mesquita B, Lopes I, Silva S, et al. Gold nanorods induce early embryonic developmental delay and lethality in zebrafish (Danio rerio). *J Toxicol Environ Health A*. 2017;80(13–15):672–687. doi:10.1080/15287394.2017.1331597

8. He A, Kwatra SG, Zampella JG, Loss MJ. Nephrogenic systemic fibrosis: fibrotic plaques and contracture following exposure to gadolinium-based contrast media. *BMJ Case Rep*. 2016;2016. doi:10.1136/bcr-2015-212769
9. Pagano G, Aliberti F, Guida M, et al. Rare earth elements in human and animal health: state of art and research priorities. *Environ Res*. 2015;142:215–220. doi:10.1016/j.envres.2015.06.039
10. Farouk M, Abd El-Maboud A, Ibrahim M, Ratep A, Kashif I. Optical properties of Lead bismuth borate glasses doped with neodymium oxide. *Spectrochim Acta a Mol Biomol Spectrosc*. 2015;149:338–342. doi:10.1016/j.saa.2015.04.070
11. Hill AJ, Teraoka H, Heideman W, Peterson RE. Zebrafish as a model vertebrate for investigating chemical toxicity. *Toxicol Sci*. 2005;86 (1):6–19. doi:10.1093/toxsci/kfi110
12. Kimmel CB, Ballard WW, Kimmel SR, Ullmann B, Schilling TF. Stages of embryonic development of the zebrafish. *Dev Dyn*. 1995;203(3):253–310. doi:10.1002/aja.1002030302
13. Jia XE, Ma K, Xu T, et al. Mutation of kri1l causes definitive hematopoiesis failure via PERK-dependent excessive autophagy induction. *Cell Res*. 2015;25(8):946–962. doi:10.1038/cr.2015.81
14. Lee KJ, Browning LM, Nallathamby PD, Xu XH. Study of charge-dependent transport and toxicity of peptide-functionalized silver nanoparticles using zebrafish embryos and single nanoparticle plasmonic spectroscopy. *Chem Res Toxicol*. 2013;26(6):904–917. doi:10.1021/tx400087d
15. Browning LM, Lee KJ, Huang T, Nallathamby PD, Lowman JE, Xu XH. Random walk of single gold nanoparticles in zebrafish embryos leading to stochastic toxic effects on embryonic developments. *Nanoscale*. 2009;1(1):138–152. doi:10.1039/b9nr00053d
16. Martino C, Costa C, Roccheri MC, Koop D, Scudiero R, Byrne M. Gadolinium perturbs expression of skeletogenic genes, calcium uptake and larval development in phylogenetically distant sea urchin species. *Aquat Toxicol*. 2018;194:57–66. doi:10.1016/j.aquatox.2017.11.004
17. Martino C, Chiarelli R, Bosco L, Roccheri MC. Induction of skeletal abnormalities and autophagy in Paracentrotus lividus sea urchin embryos exposed to gadolinium. *Mar Environ Res*. 2017;130:12–20. doi:10.1016/j.marenvres.2017.07.007
18. Welsh DG, Nelson MT, Eckman DM, Brayden JE. Swelling-activated cation channels mediate depolarization of rat cerebrovascular smooth muscle by hyposmolarity and intravascular pressure. *J Physiol*. 2000;527 Pt 1:139–148. doi:10.1111/tjp.2000.527.issue-1
19. Akre BT, Dunkel JA, Hustvedt SO, Refsum H. Acute cardiotoxicity of gadolinium-based contrast media: findings in the isolated rat heart. *Acad Radiol*. 1997;4(4):283–291. doi:10.1016/S1076-6332(97)80030-X
20. Saghiri MA, Orangi J, Asatourian A, Sorenson CM, Sheibani N. Functional role of inorganic trace elements in angiogenesis part III: (Ti, Li, Ce, As, Hg, Va, Nb and Pb). *Crit Rev Oncol Hematol*. 2016;98:290–301. doi:10.1016/j.critrevonc.2015.10.004
21. Giri S, Karakoti A, Graham RP, et al. Nanoceria: a rare-earth nanoparticle as a novel anti-angiogenic therapeutic agent in ovarian cancer. *PLoS One*. 2013;8(1):e54578. doi:10.1371/journal.pone.0054578
22. Zheng Y, Wu Z, Yi F, et al. By activating Akt/eNOS bilobalide B inhibits autophagy and promotes angiogenesis following focal cerebral ischemia reperfusion. *Cell Physiol Biochem*. 2018;47 (2):604–616. doi:10.1159/000490016
23. Du J, Teng RJ, Guan T, et al. Role of autophagy in angiogenesis in aortic endothelial cells. *Am J Physiol Cell Physiol*. 2012;302(2): C383–C391. doi:10.1152/ajpcell.00164.2011
24. Carmeliet P, Tessier-Lavigne M. Common mechanisms of nerve and blood vessel wiring. *Nature*. 2005;436(7048):193–200. doi:10.1038/nature03875
25. Eichmann A, Le Noble F, Autiero M, Carmeliet P. Guidance of vascular and neural network formation. *Curr Opin Neurobiol*. 2005;15(1):108–115. doi:10.1016/j.conb.2005.01.008
26. Mikhailova MM, Panteleyev AA Jr., Paltsev MA, Panteleyev AA. Spinal cord tissue affects sprouting from aortic fragments in ex vivo co-culture. *Cell Biol Int*. 2019. doi:10.1002/cbin.11112
27. Huang LH, Yang H, Su X, Gao YR, Xue HN, Wang SH. Neodymium oxide induces cytotoxicity and activates NF-kappaB and Caspase-3 in NR8383 cells. *Biomed Environ Sci*. 2017;30(1):75–78. doi:10.3967/bes2017.010
28. Lu VM, Crawshay-Williams F, White B, Elliot A, Hill MA, Townley HE. Cytotoxicity, dose-enhancement and radiosensitization of glioblastoma cells with rare earth nanoparticles. *Artif Cells Nanomed Biotechnol*. 2019;47(1):132–143. doi:10.1080/21691401.2018.1544564
29. Zhang Y, Yu C, Huang G, Wang C, Wen L. Nano rare-earth oxides induced size-dependent vacuolization: an independent pathway from autophagy. *Int J Nanomedicine*. 2010;5:601–609. doi:10.2147/IJN.S11513
30. Yu L, Lu Y, Man N, Yu SH, Wen LP. Rare earth oxide nanocrystals induce autophagy in HeLa cells. *Small*. 2009;5(24):2784–2787. doi:10.1002/smll.200901714
31. Yang T, Wu T, Lv L, et al. Ceria oxide nanoparticles an ideal carrier given little stress to cells and rats. *J Nanosci Nanotechnol*. 2018;18 (6):3865–3869. doi:10.1166/jnn.2018.15018
32. Hussain S, Al-Nsour F, Rice AB, et al. Cerium dioxide nanoparticles induce apoptosis and autophagy in human peripheral blood monocytes. *ACS Nano*. 2012;6(7):5820–5829. doi:10.1021/nn302235u
33. Alarifi S, Ali H, Alkahtani S, Alessia MS. Regulation of apoptosis through bcl-2/Bax proteins expression and DNA damage by nano-sized gadolinium oxide. *Int J Nanomedicine*. 2017;12:4541–4551. doi:10.2147/IJN.S139326
34. Hosseini A, Sharifi AM, Abdollahi M, et al. Cerium and yttrium oxide nanoparticles against lead-induced oxidative stress and apoptosis in rat hippocampus. *Biol Trace Elem Res*. 2015;164(1):80–89. doi:10.1007/s12011-014-0197-z